Metal Hydrides

International Edition: DOI: 10.1002/anie.201604308
German Edition: DOI: 10.1002/ange.201604308

CO_2 Activation and Hydrogenation by PtH_n^- Cluster Anions

*Xinxing Zhang, Gaoxiang Liu, Karl-Heinz Meiwes-Broer, Gerd Ganteför, and Kit Bowen**

Abstract: *Gas phase reactions between PtH_n^- cluster anions and CO_2 were investigated by mass spectrometry, anion photoelectron spectroscopy, and computations. Two major products, $PtCO_2H^-$ and $PtCO_2H_3^-$, were observed. The atomic connectivity in $PtCO_2H^-$ can be depicted as $HPtCO_2^-$, where the platinum atom is bonded to a bent CO_2 moiety on one side and a hydrogen atom on the other. The atomic connectivity of $PtCO_2H_3^-$ can be described as $H_2Pt(HCO_2)^-$, where the platinum atom is bound to a formate moiety on one side and two hydrogen atoms on the other. Computational studies of the reaction pathway revealed that the hydrogenation of CO_2 by PtH_3^- is highly energetically favorable.*

The transformation of carbon dioxide into reduced, higher value molecules, such as methanol and formic acid, is of great interest for both environmental and economic reasons. In solution, ligand-protected transition metal hydride complexes, L_nMH, often play important roles in these processes.[1–19] The critical reduction step involves the insertion of the C=O group of carbon dioxide into the M–H bond to produce a formate–metal adduct, L_nM-OC(O)H, from which the formate product can be generated. There are, on the other hand, fewer reports of CO_2 reduction by ligandless metal hydrides. Those studies that have been conducted include the methanation of CO_2 on Mg_2NiH_4 surfaces[20] and similar reactions on hydrogen-loaded $LaNi_5$ and $LaNi_4Cr$ surfaces, where their hydrides play critical roles.[21] Gas phase work is even rarer. While naked (ligandless) transition metal hydrides have been generated in the gas phase as both positive and negative ions (for example, FeD^+, CoD^+, NiD^+, CrH^-, NiH^-, CoH^-, CuH^-, and FeH_2^-)[22–25] we are not aware of them being utilized in CO_2 reactivity studies. However, a recent report details the gas phase, ligand-protected, activation of CO_2 by a Cp_2TiH^+ metal hydride cation.[19]

The present work focuses on the hydrogenation of CO_2 via reactions with platinum hydride cluster anions, PtH_n^-. Platinum hydride cluster anions were chosen because platinum is an excellent hydrogenation catalyst, their hydrides are good sources of hydrogen, and their excess negative charges promote the activation of CO_2. The two products of these reactions, $PtCO_2H^-$ and $PtCO_2H_3^-$, were identified by mass spectrometry and characterized by anion photoelectron spectroscopy. Ab initio computational studies of the mechanistic pathway revealed that the hydrogenation of CO_2 by PtH_3^- is strongly favorable energetically.

The details of experimental and computational methods are provided in the Supporting Information. The mass spectra with or without CO_2 pulsed into the reaction cell are shown in Figure 1. With no CO_2 in the cell, only PtH_n^- cluster anions were observed in the mass spectrum (Figure 1 A; Supporting Information, Figure S1). Individual PtH_n^- species were identified by recording anion photoelectron spectra at every mass peak in the series. These spectra are shown in Figure S1 (Supporting Information), beginning at 194 amu and continuing in single amu steps up to 203 amu. (Mass 202 is missing in the mass spectrum, indicating that PtH_4^- is not present.) The photoelectron spectrum at mass 194 was identified as the well-known photoelectron spectrum of Pt^-. As well as Pt^- peaks from another Pt^- isotope, new peaks in the photoelectron spectrum at mass 195 are due to PtH^-. New peaks on top of those in the photoelectron spectrum at mass 196 are due to PtH_2^-, and so on, up to PtH_5^-. No PtH_4^- was present.

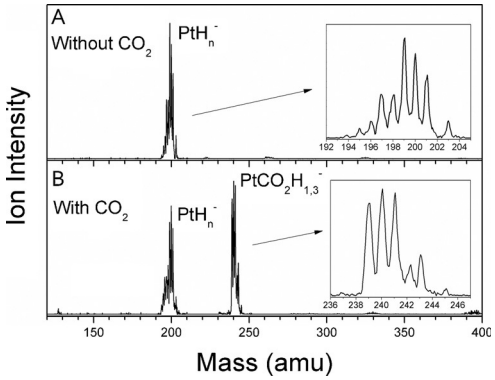

Figure 1. The mass spectra of PtH_n^- cluster anions A) without and B) with CO_2 injection into the cell.

When CO_2 was added to the cell, the ion intensity of the PtH_n^- series decreased, and a new series of $PtCO_2H_m^-$ cluster anions appeared (Figure 1 B). No other products were observed in the entire mass spectrum. The lowest mass peak at 239 amu is due to $PtCO_2H^-$, while the highest mass peak at 245 amu is due to $PtCO_2H_3^-$; hence, $PtCO_2H^-$ and $PtCO_2H_3^-$ coexist in the ion beam. Since there is essentially no mass peak at 244 amu, we are confident that $PtCO_2H_2^-$ is not present in the beam. The intensity of $PtCO_2H_3^-$ is calculated

[*] Dr. X. Zhang, G. Liu, Prof. Dr. K. Bowen
Department of Chemistry, Johns Hopkins University
3400 N. Charles Street, Baltimore, MD 21218 (USA)
E-mail: kbowen@jhu.edu
Prof. Dr. K. Meiwes-Broer
Institut für Physik, Universität Rostock
Albert-Einstein-Str. 24, 18059 Rostock (Germany)
Prof. Dr. G. Ganteför
Fachbereich Physik, Universität Konstanz
Fach: 690, 78457 Konstanz (Germany)

Supporting information for this article can be found under: http://dx.doi.org/10.1002/anie.201604308.

to be 29% of that of $PtCO_2H^-$ (Supporting Information, Figure S2). More detailed mass spectral and photoelectron spectral analysis of the $PtCO_2H^-$ and $PtCO_2H_3^-$ cluster anions are presented in Figure S2 and S3 (Supporting Information). Note that both $PtCO_2H^-$ and $PtCO_2H_3^-$ have closed-shell electron configurations.

The photoelectron spectrum of $PtCO_2H_3^-$ is presented in Figure 2, and was measured with the third harmonic output of a Nd:YAG laser (3.496 eV). It was recorded at mass 245 amu to ensure that the resulting photoelectron signal was primarily due to $PtCO_2H_3^-$. This spectrum is dominated by a band that ranges from electron binding energy (EBE) = 3.0 to 3.5 eV,

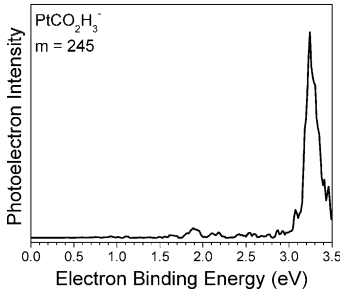

Figure 2. Photoelectron spectrum of $PtCO_2H_3^-$ taken at mass 245 with 355 nm (3.496 eV) photons.

with a maximal spectral intensity at EBE = 3.24 eV. Thus, 3.24 eV is the vertical detachment energy (VDE) value for $PtCO_2H_3^-$, that is, the transition energy at which the Franck-Condon overlap is at its maximum between the anion's wave function and that of its neutral counterpart. The electron affinity (EA) is the energy difference between the relaxed ground state of the anion, and the relaxed ground state of its neutral counterpart. The EA value for $PtCO_2H_3$ is estimated to be 3.1 eV by extrapolating the lower EBE side of the band to zero photoelectron intensity. The small peak at EBE = 3.08 eV and other very weak features at the low EBE side of the main band are due to the much less abundant isotopomer of $PtCO_2H^-$ at mass = 245 (Supporting Information, Figure S2).

The photoelectron spectrum of $PtCO_2H^-$ is shown in Figure 3C. With five spectral bands in evidence, it is more complicated than that of $PtCO_2H_3^-$. Its features are due, not only to the photodetachment of $PtCO_2H^-$, but also to the photodissociation of $PtCO_2H^-$ into PtH^- and CO_2, followed by photodetachment of the resultant anion, PtH^-. The latter is a two-photon process, where one photon is absorbed, inducing fragmentation, while another photon photodetaches the anionic product of dissociation. This can be seen by comparing the photoelectron spectrum of $PtCO_2H^-$ with that of PtH^-. Unfortunately, we did not observe the photoelectron spectrum of PtH^- by itself in these experiments. This was because every isotopic mass peak of PtH^- overlaps with at least one of the following anions: Pt^-, PtH_2^-, or PtH_3^-. Nevertheless, we were still able to identify the photoelectron spectral transitions in PtH^- by comparing the photoelectron spectra at mass = 194 (Pt^-; Figures 3A) with that at mass = 195 (a combination of Pt^- and PtH^-; 3B). In the

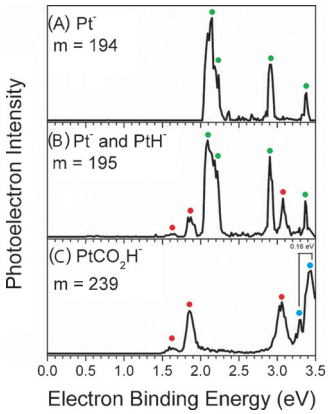

Figure 3. Photoelectron spectra of A) Pt^- (●) taken at mass = 194; B) Pt^- (●) and PtH^- (●) taken at mass = 195; C) PtH^- (●) and $PtCO_2H^-$ (●) taken at mass = 239.

photoelectron spectrum for mass 195 (Figure 3B), Pt^- peaks at EBE = 2.1, 2.2, 2.9, and 3.4 eV (green dots) share the spectrum with three additional peaks at EBE = 1.60, 1.85, and 3.08 eV (red dots); these are due to PtH^-. Significantly, the latter peaks reappear in the photoelectron spectrum of $PtCO_2H^-$ in Figure 3C, not only at the same EBE positions, but also with nearly identical relative intensities. It is clear that the peaks denoted by red dots in the photoelectron spectrum of $PtCO_2H^-$ are due to PtH^-. $PtCO_2H^-$ has undergone both photodetachment and photodissociation.

As an aside, the embedded photoelectron spectrum of PtH^- has allowed us to determine, for the first time, that the VDE value of PtH^- is 1.60 eV and the EA value of PtH is 1.5 eV. While the photoelectron study of PtH_n^- was not an explicit goal of this work, it does add to the mosaic of accumulated data on transition metal hydrides.

The photoelectron spectrum of $PtCO_2H^-$ resides on the high EBE side of Figure 3C as two peaks (blue dots), a small peak at EBE = 3.30 eV and a broader band that reaches its maximum photoelectron intensity at EBE = 3.46 eV. Thus, 3.46 eV is the VDE value for $PtCO_2H^-$. We further assign its EA value as 3.30 eV. The spacing between these two peaks is 0.16 eV, which is very close to the 1280 cm^{-1} C–O stretching frequency that we calculated for $PtCO_2H$. This value is consistent with a weakening of the C–O bond caused by the activation of the CO_2 moiety. Based on photodissociation products of $PtCO_2H^-$ (PtH^- and CO_2 inferred), we speculate that the structure of $PtCO_2H^-$ consists of a CO_2 moiety and a PtH^- moiety. As seen below, our computations bear that expectation out.

Figure 4 presents the optimized structures of $PtCO_2H^-$ and $PtCO_2H_3^-$. The calculated 3D coordinates of these two products are provided in the Supporting Information. For $PtCO_2H_3^-$, the global minimum is found to have C_{2v} symmetry. It can be viewed as a formate anion/PtH_2 adduct, namely $H_2Pt(HCO_2)^-$, where the platinum atom is planar tetra-coordinated (PTC) by two hydrogen atoms and the two oxygen atoms of the formate anion moiety. A PTC structure is stable and commonly seen in platinum-containing molecules. Natural Population Analysis (NPA) shows that, along with

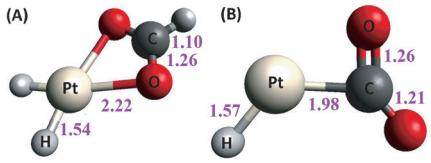

Figure 4. A) Optimized structures of $PtCO_2H_3^-$ and B) $PtCO_2H^-$. Bond lengths (Å).

CO_2 insertion and hydrogen atom migration, charge is also transferred from the platinum hydride anion to CO_2, making the formate anion moiety negatively charged by $-0.77\,e$.

In the optimized structure of $PtCO_2H^-$, the only hydrogen atom is bonded to platinum. The platinum atom also bonds to the carbon atom of the CO_2 moiety, which is bent from its original linear structure, indicating that CO_2 has been activated by PtH^-. This structure is consistent with photodissociation evidence observed in the photoelectron spectrum. NPA shows that the negative charge is also partially transferred from PtH^- to CO_2, resulting in a total charge of $-0.66\,e$ on the CO_2 moiety. The O-C-O bond angle is determined to be 139.5°, close to the 134° bond angle of the free CO_2^- anion at its global minimum.[26–28] This indicates that, even though hydrogenation of the CO_2 moiety does not occur, CO_2 nevertheless becomes activated by its interaction with PtH^-. The behavior of PtH^- is analogous to that of Au^-, its isoelectronic analogue, which is known to activate CO_2 by charge transfer.[29,30]

Table 1 presents the EA and VDE values of $PtCO_2H$/$PtCO_2H^-$ and $PtCO_2H_3$/$PtCO_2H_3^-$ calculated at different theory levels. Agreement among different levels of theory is very good, and is also excellent between the calculated and experimental values.

Table 1: Experimental and calculated VDE/EA values for $PtCO_2H$/$PtCO_2H^-$ and $PtCO_2H_3$/$PtCO_2H_3^-$.

VDE/EA values [eV]	$PtCO_2H_3$/$PtCO_2H_3^-$	$PtCO_2H$/$PtCO_2H^-$
Experimental	3.24/3.10	3.46/3.30
UPBE0	3.37/3.21	3.55/3.23
CCSD	3.10/2.94	3.38/3.28
CCSD(T)	3.19/2.94	3.46/3.44

DFT calculations were carried out to investigate the mechanism of CO_2 activation and hydrogenation. The reaction pathways were calculated for the reactions of PtH^- and PtH_3^- with CO_2, respectively. The pathway of CO_2 hydrogenation by PtH_3^- is presented in Figure 5. Before reaction, PtH_3^- exhibits C_{2v} symmetry. The first step in the reaction is CO_2 activation by charge transfer from PtH_3^-. As soon as CO_2 approaches the platinum atom, it bends, and the energy drops by 0.61 eV (structure 1a). The highest occupied molecular orbital (HOMO) of structure 1a (Figure 5) indicates that the excess electron density is delocalized over the entire cluster. Furthermore, according to NPA, the net charge on the CO_2 moiety is $-0.39\,e$, showing that it has been significantly activated. After activation, the CO_2 moiety is

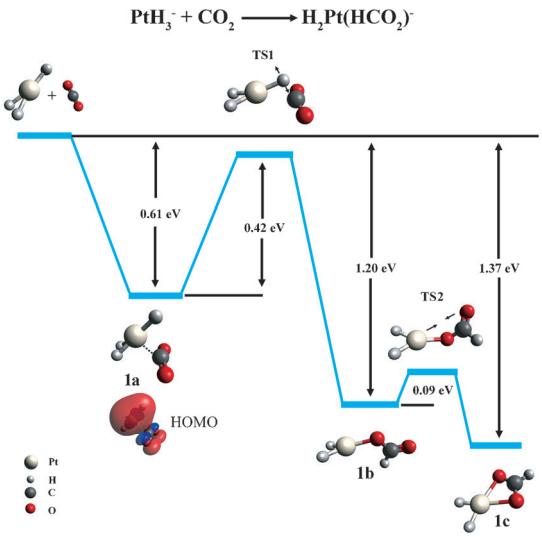

Figure 5. Calculated reaction pathway for CO_2 hydrogenation by PtH_3^-.

ready to accept a hydrogen atom from PtH_3^-. The insertion of CO_2 into the Pt–H bond passes through the first transition state (structure TS1), with an energy barrier of 0.42 eV. Once the hydrogen atom has transferred to CO_2, hydrogenation is complete, yielding structure 1b (a local minima). Structure 1b must overcome a small rotational barrier (0.09 eV, TS2) so that $PtCO_2H_3^-$ may reach the global minimum structure shown in Figure 4A (that is, structure 1c in Figure 5). This permits the other oxygen atom to coordinate with the platinum atom, further stabilizing the entire cluster.

The potential energy pathway for the reaction between CO_2 and PtH^- is presented in Figure 6. As in the first step in the reaction between CO_2 and PtH_3^-, CO_2 is also activated in this case by charge transfer with the platinum atom, forming a bond between the platinum and carbon atoms (structure 2a). The HOMO of this structure also shows substantial delocalization. The activation of CO_2 provides 1.70 eV of stabilization energy to structure 2a of $PtCO_2H^-$. (Interestingly, this is much larger than the analogous stabilization energy for CO_2 activation in $PtCO_2H_3^-$, which is

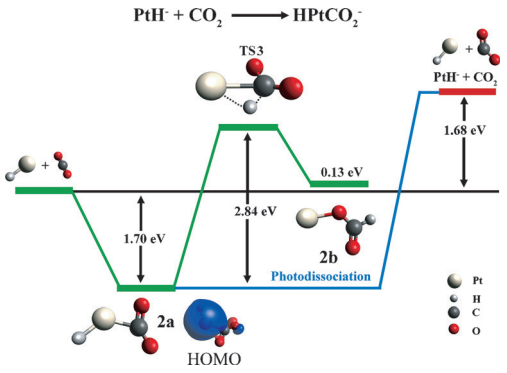

Figure 6. Calculated reaction pathway for CO_2 activation and thwarted hydrogenation by PtH^-. The photodissociation process of $PtCO_2H^-$ is also presented.

0.61 eV.) Nevertheless, even though CO_2 activation has been achieved at this point in the CO_2 and PtH^- pathway (via structure 2a), the reaction cannot proceed further to CO_2 hydrogenation. The reason that the reaction stops at this juncture is because of 2.84 eV energy barrier, against which hydrogen atom transfer from structure 2a to TS3 would have to occur. (Again, this energy is much higher than the analogous 0.42 eV barrier in the CO_2 and PtH_3^- reaction.) The reaction cannot proceed to structure 2b. Our photoelectron spectrum of $PtCO_2H^-$ and accompanying calculations imply that we have made and photodetached structure 2a, rather than structure 2b. Figure 6 also shows the energy needed to photodissociate structure 2a into $PtH^- + CO_2$ (that is, 1.70 eV + 1.68 eV = 3.38 eV). We irradiated $PtCO_2H^-$ with 3.496 eV photons when measuring the photoelectron spectrum, which is only slightly more energy than what is required to dissociate $PtCO_2H^-$. Everything that we deduced from Figure 3C is consistent with the energetics presented in Figure 6, in terms of the photodetachment and the photodissociation of $PtCO_2H^-$.

Lastly, while there is some evidence that PtH_5^- existed in the ion beam (Supporting Information, Figure S1), there is no evidence that it reacted with CO_2; no $PtCO_2H_5^-$ was observed in the mass spectrum. The reasons for the inertness of PtH_5^- toward CO_2 may be both structural and electronic. PtH_5^- exhibits D_{5h} symmetry. Thus, since the platinum atom is surrounded by hydrogen atoms, it is difficult for CO_2 to gain access to the platinum atom. Furthermore, PtH_5^- is a very stable species because of σ-aromatic bonding. Both geometric and electronic features of PtH_5^- are highlighted in Figure S4 (Supporting Information). Our calculations also show that PtH_5^- and CO_2 do not react.

Acknowledgements

This material is based upon work supported by the National Science Foundation (NSF) under Grant No. CHE-1360692 and by the Air Force Office of Scientific Research (AFOSR), under Grant No. FA9550-15-1-0259.

Keywords: ab initio calculations · anion photodetachment · carbon dioxide fixation · metal hydrides

How to cite: *Angew. Chem. Int. Ed.* **2016**, *55*, 9644–9647
Angew. Chem. **2016**, *128*, 9796–9799

[1] P. G. Jessop, T. Ikariya, R. Noyori, *Chem. Rev.* **1995**, *95*, 259–272.
[2] M. S. Jeletic, M. L. Helm, E. B. Hulley, M. T. Mock, A. M. Appel, J. C. Linehan, *ACS Catal.* **2014**, *4*, 3755–3762.
[3] M. A. Rankin, C. C. Cummins, *J. Am. Chem. Soc.* **2010**, *132*, 10021–10023.
[4] A. J. M. Miller, J. A. Labinger, J. E. Bercaw, *Organometallics* **2011**, *30*, 4308–4314.
[5] B. P. Sullivan, T. J. Meyer, *J. Chem. Soc. Chem. Commun.* **1984**, *1984*, 1244–1245.
[6] M. K. Whittlesey, R. N. Perutz, M. H. Moore, *Organometallics* **1996**, *15*, 5166–5169.
[7] P. Kang, C. Cheng, Z. Chen, C. K. Schauer, T. J. Meyer, M. Brookhart, *J. Am. Chem. Soc.* **2012**, *134*, 5500–5503.
[8] D. J. Darensbourg, A. Rokicki, M. Y. Darensbourg, *J. Am. Chem. Soc.* **1981**, *103*, 3223–3224.
[9] D. L. DuBois, D. E. Berning, *Appl. Organomet. Chem.* **2000**, *14*, 860–862.
[10] J. R. Pugh, M. R. M. Bruce, B. P. Sullivan, T. J. Meyer, *Inorg. Chem.* **1991**, *30*, 86–91.
[11] S. E. Clapham, A. Hadzovic, R. H. Morris, *Coord. Chem. Rev.* **2004**, *248*, 2201–2237.
[12] W. Leitner, *Angew. Chem. Int. Ed. Engl.* **1995**, *34*, 2207–2221; *Angew. Chem.* **1995**, *107*, 2391–2405.
[13] S. Saeidi, N. A. S. Amin, M. R. Rahimpour, *J. CO2 Utilization* **2014**, *5*, 66–81.
[14] H. Arakawa et al., *Chem. Rev.* **2001**, *101*, 953–996.
[15] M. Aresta, A. Dibenedetto, *Dalton Trans.* **2007**, *28*, 2975–2992.
[16] G. Fachinetti, C. Floriani, A. Roselli, S. Pucci, *J. Chem. Soc. Chem. Commun.* **1978**, *6*, 269–270.
[17] S. Gambarotta, S. Strologo, C. Floriani, A. Chiesi-Villa, C. Guastini, *J. Am. Chem. Soc.* **1985**, *107*, 6278–6282.
[18] A. Cutler, M. Raja, A. Todaro, *Inorg. Chem.* **1987**, *26*, 2877–2881.
[19] S. Tang, N. J. Rijs, J. Li, M. Schlangen, H. Schwarz, *Chem. Eur. J.* **2015**, *21*, 8483–8490.
[20] S. Kato, A. Borgschulte, D. Ferri, M. Bielmann, J. C. Crivello, D. Wiedenmann, M. Parlinska-Wojtan, P. Rossbach, Y. Lu, A. Remhof, A. Züttel, *Phys. Chem. Chem. Phys.* **2012**, *14*, 5518–5526.
[21] K. Soga, K. Otsuka, M. Sato, T. Sano, S. Ikede, *J. Less-Common Met.* **1980**, *71*, 259–263.
[22] T. J. Carlin, L. Sallans, C. J. Cassady, D. B. Jacobson, B. S. Freiser, *J. Am. Chem. Soc.* **1983**, *105*, 6320–6321.
[23] A. E. S. Miller, C. S. Feigerle, W. C. Lineberger, *J. Chem. Phys.* **1986**, *84*, 4127–4131.
[24] A. E. S. Miller, C. S. Feigerle, W. C. Lineberger, *J. Chem. Phys.* **1987**, *87*, 1549–1556.
[25] R. M. D. Calvin, D. H. Andrews, W. C. Lineberger, *Chem. Phys. Lett.* **2007**, *442*, 12–16.
[26] R. N. Compton, P. W. Reinhardt, C. D. Cooper, *J. Chem. Phys.* **1975**, *63*, 3821.
[27] M. Knapp, O. Echt, D. Kreisle, T. D. Mark, E. Recknagel, *Chem. Phys. Lett.* **1986**, *126*, 225–231.
[28] S. T. Arnold, J. V. Coe, J. G. Eaton, C. B. Freidhoff, L. H. Kidder, G. H. Lee, M. R. Manaa, K. M. McHugh, D. Patel-Misra, H. W. Sarkas, J. T. Snodgrass, K. H. Bowen, in *Proceedings of the Enrico Fermi International School of Physics, CVII Course, Varenna*, (Eds.: G. Scoles) North-Holland, Amsterdam, **1989**, pp. 467–490.
[29] X. Zhang, E. Lim, S. K. Kim, K. H. Bowen, *J. Chem. Phys.* **2015**, *143*, 174305.
[30] A. D. Boese, H. Schneider, A. N. Gloess, J. M. Weber, *J. Chem. Phys.* **2005**, *122*, 154301.

Received: May 3, 2016
Revised: June 7, 2016
Published online: July 1, 2016

